

# Fault Diagnosis and Fault-Tolerant Control Scheme for Open-Circuit Faults in Three-Stepped Bridge Converters

Cheng Shu, Li Wei, Ding Rong-Jun, and Chen Te-Fang

**Abstract**—A novel fault diagnosis method and a fault tolerant scheme for open-circuit faults on a traction rectifier are proposed in this paper. When an open-circuit fault occurs in any leg of the rectifier, indication will be generated accurately to identify the faulty leg without utilization of any extra sensors. Furthermore, the faulty rectifier can be reconfigured to maintain its full output rate to prevent traction rectifier breakdown. The fault diagnosis process is neither related to control trigger signal nor the load fluctuation. The involved parameters are the input and output voltage of the rectifier, which are the most common parameters in rectifier control. Working under zero voltage and zero current, five additional switch sets are adopted for the fault-tolerant control process to reconfigure the topological structure between the traction rectifier and the traction transformer, meanwhile the original structure of the rectifier is retained. Analysis, design, and implementing consideration for both normal and abnormal operating situations of the traction rectifier are present in this paper. The experiment is processed to verify the effectiveness of the theoretical analysis.

**Index Terms**—Fault diagnosis, fault location, fault tolerance, rectifiers.

## I. INTRODUCTION

NOWADAYS, considerable locomotives powered by dc motors are still on active service worldwide, for example, there are thousands of dc motor-powered locomotives operating continuously in railways, mines, and factories in China. These locomotives normally have relatively longer service time and higher risk of converter breakdown. Meanwhile, the fault monitoring and diagnosis are much more trivial than that of the modern ac traction locomotives. The fault statistics for one certain type of locomotive in a corporation in the second quarter of year 2015 in China are shown in Table I. There are nine converter failures accounting for 42.86% of total locomotive failures, which makes converter become the most vulnerable key electric subsystem. Due to the destructiveness and high rate

Manuscript received April 22, 2015; revised February 28, 2016; accepted April 14, 2016. Date of publication April 27, 2016; date of current version December 9, 2016. This work was supported in part by the National Natural Science Foundation of China under Grant 61273158. Recommended for publication by Associate Editor H. Wang.

C. Shu and C. Te-Fang are with the Institute of Rail Transport and Electric Traction Technology, Changsha 410075, China, and the School of Traffic and Transportation Engineering, Central South University, Changsha 410075, China (e-mail: chengshu@csu.edu.cn; ctfeyt@163.com).

L. Wei is with CSR Zhuzhou Institute Co. Ltd, Zhuzhou 412001, China, and also with the School of Traffic and Transportation Engineering, Central South University, Changsha 410075, China (e-mail: liwei\_china@sina.com).

D. Rong-Jun is with CSR Zhuzhou Institute Co. Ltd, Zhuzhou 412001, China, and also with the Chinese Academy of Engineering, Beijing 100088, China (e-mail: dingrj@teg.cn).

Digital Object Identifier 10.1109/TPEL.2016.2558491

TABLE I  
STATISTICS OF LOCOMOTIVE FAILURE IN THE SECOND QUARTER OF YEAR 2015

Category	Break System	Main Transformer	Control System	Converter	Brake System
Amount	0	1	1	9	1
Ratio	0	4.76%	4.76%	42.86%	4.76%
Category	Battery	Electronics	Other Devices	Sum	
Amount	1	2	6	21	
Ratio	4.76%	9.52%	28.57%	100%	

of traction converter failures, it has been paid more attention recently.

Many research works have been conducted which are related to the fault diagnosis and fault tolerance control on converters recently. Diagnosis methods that aim at rectifiers, inverters, dc-dc converters, and key components are discussed in categories. The fault diagnosis methods on a rectifier are discussed in [1]–[3]. Based on the observation of the chopped bus current, the authors in [1] introduce a fault locating method for thyristor open-switch fault in a rectifier. This method needs two extra current sensors that may subsequently increase potential failure point and cost. Only the phase current is used to diagnose both open- and short-circuit fault in [2], but in order to locate the faulty switches, a specific test has to be performed according to the fault type. Another drawback is the possibility of not being able to locate faulty switches in a certain period; these two drawbacks make this method not suitable for online diagnosis. In [3], a real-time diagnosis method is proposed for open-circuited and unbalance faults in residential small wind systems grid-tied converters, the spectrum and dc components analysis of the voltage and current is utilized for the fault locating and unbalance input voltage detecting. The computational complexity is relatively large and a high performance processor is needed to ensure the efficiency of this method. Inverter fault diagnosis methods are discussed in [4]–[14]. A voltage-based approach for open-circuit fault diagnosis in closed-loop-controlled pulse width modulation (PWM) converters is proposed in [4]. This method does not need any additional sensors. On the other hand, at least some lines have to be added to the original inverter to collect the reference signal, since a lot of safety critical application do not allow any modification on the original system, or rigorous tests and verification must be taken to prove that the modification is useful and harmless to the reliability of the original system,

this may require the inverter to do offline tests for months, and the cost may be expensive. An algorithm for multiple open-circuit faults diagnosis in full-scale back-to-back converters is presented in [5]. The phase current is adopted and processed to be independent under operating conditions, but the performance of the method strongly relies on the selection of the empirically thresholds, so the consistency of the method's effectiveness cannot be guaranteed. An open-circuit switch fault detection method and a diagnosis system for matrix converters are presented in [6]. No load models, averaging windows, or additional sensors are needed for this method, but adjustment to the original converter is required as well as the switch state. An extension of the normalized dc-components-based diagnosis method is proposed in [7]. A d-q voltage offset observer is designed to detect open-switch fault in [8]. The authors in [9] present a Concordia current pattern radius-based method. In [10], a suitable method which is integrated into the drive controller is proposed, and it can trigger remedial actions. Relatively complex calculation is needed by [7]–[10] which may increase the system complexity and cost. The voltage difference of lower switches between faulty and normal states is used in [11]. The difference of the line voltage between on and off state within one PWM period is adopted in [12]; PWM switching signals and the line-to-line voltage levels during the switching times in voltage source inverter-fed induction motor drives are analyzed in [13]. This method achieves not only accurate single and multiple switches fault diagnosis but also minimization of the fault detection time, which is maximum one switching period. The authors in [11]–[13] need a trigger signal as diagnosis eigenvalue, so there must be some modifications on the inverter controller, which may lead to additional time and expense cost on the modified inverter's approval. Four detection techniques of voltage-fed asynchronous machine drive systems have been introduced and compared in [14]. Fault diagnosis methods of the dc-dc converter are discussed in [15]–[16]. By using the dc-link current and transformer primary voltage as the diagnosis criteria, a switch short-circuit fault diagnostic method is proposed for the dc-dc full-bridge converter in [15], but this method needs switch gate-driver signals to perform diagnosis, and needs additional hardware to achieve fault-tolerance control. In [16], the slope of the inductor current is adopted as the diagnosis value and is observed over time. A hybrid structure of two parallel working FD subsystems is also adopted to fast diagnosis. Fault states of key components are also vital to the converter as discussed in [17]–[20]. Reliability of power electronic systems is characterized into three main aspects in [21]. On the grounds of fault diagnosis, several fault-tolerance control methods are present in [13], and [22]–[23].

All methods mentioned above have advantages in specific applications, but do not fit well in traction converters application. A new fault diagnosis method and a fault-tolerance control scheme are proposed with minimal system modification and no use of empirically parameters; no additional sensors are needed; the diagnosis process is independent of any controller's signal and load fluctuation; the diagnosis process can be carried out within two or less systematic working cycles while rectifier's normal operation is not interrupted. The proposed diagnosis

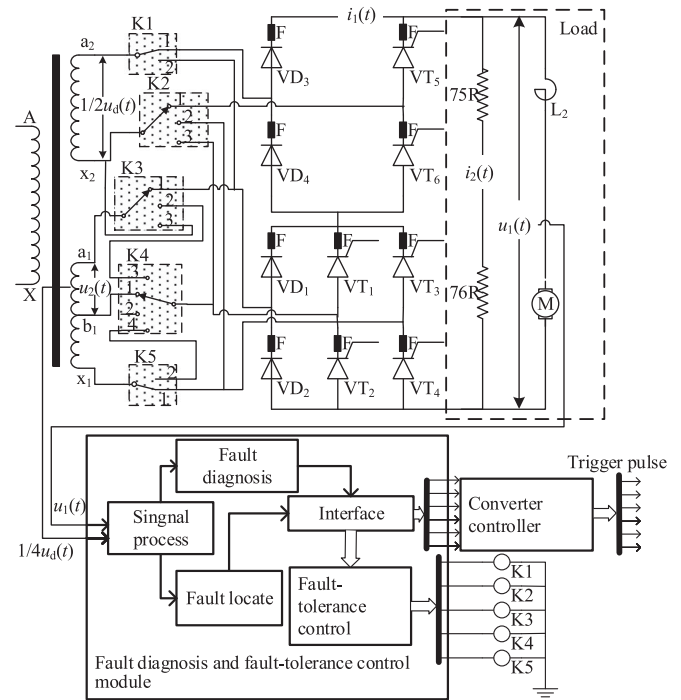


Fig. 1. Topology of the proposed system.

system can be treated as a completely independent device to the objective rectifier, so the original rectifier does not need to acquire additional approval. After fault is located, full capacity of the rectifier under one switch open-circuit fault is guaranteed and the five additional switch sets are installed outside the rectifier. Most important advantage is that the proposed method can achieve all above features at the same time.

## II. SYSTEM OVERVIEW

### A. Configuration

The three-stepped half-controlled bridge rectifier topology and the proposed system are shown in Fig. 1, where  $VD_1 \sim VD_4$  are power diodes,  $VT_1 \sim VT_6$  are thyristors,  $a_1b_1x_1$  and  $a_2x_2$  are secondary windings of the traction transformer.  $75R/76R$  are resistors used to absorb the overvoltage and free-wheel current when the rectifier is unloaded.  $L_2$  is the smoothing reactor of traction motors.  $K1-K5$  are switch sets and their coils, which are used in fault tolerance control.  $u_d(t)$  stands for the total voltage of the traction transformer's secondary windings, so voltage on  $a_2x_2$  winding is  $1/2u_d(t)$ , and voltage on  $a_1b_1$  and  $b_1x_1$  are  $1/4u_d(t)$ .  $u_1(t)$  denotes the output voltage of the rectifier.

### B. Overall Operating Principle

This paper focuses on open-circuit fault of switches, because short-circuit switches will be cutoff instantly by means of the fast fuses  $F$  in Fig. 1. The output waveforms deviation caused by the open-circuit fault can be used to locate faulty switch precisely. The proposed diagnosis and fault-tolerance control

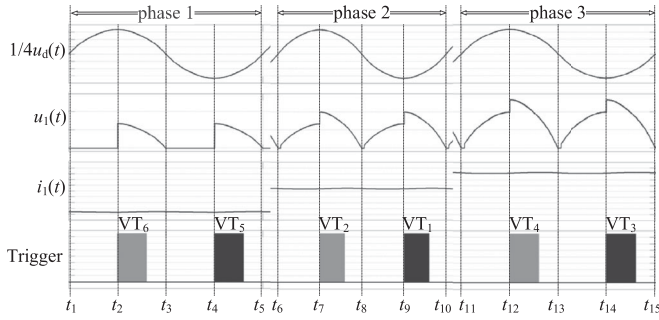


Fig. 2. System waveforms under normal operation.

method has three working stages. Key parameters of the rectifier are monitored in the first stage while the rectifier is working properly. Fault diagnosis is proceeded when open-circuit fault occurs, the faulty switch is located based on  $u_1(t)$ ,  $u_d(t)$ , and the implicit relationship between them in the second stage. Then, fault tolerance control is carried out in the third stage to keep the rectifier's full output range by switching K1-K5 and adjusting the control strategy properly.

### C. Diagnosis Signals

To ensure the practicability of the fault diagnosis and the fault tolerance control method, it is strongly desirable to choose diagnosis signals from the precollected signals of the original rectifier controller. The output voltage  $u_1(t)$  is chosen to obtain the most direct information of the rectifier state. The input voltage  $u_d(t)$  is also selected to distinguish upper switches fault from lower switches fault of the same leg. These two signals can be easily obtained without any additional sensors.

## III. FAULT DIAGNOSIS AND FAULT-TOLERANCE CONTROL

Three assumptions are made for the following analysis: 1) all components are ideal; 2) the traction motor is regarded as a combination of resistor, inductor, and back EMF; 3) the output inductor is large enough to be treated as a constant current source in a short time period; 4) the steady state is reached.

### A. Analysis of the Normal Operation

Switches  $K1 \sim K5$  are set to position 1 when the rectifier is fault-free. Fig. 2 shows the normal operation waveforms of the rectifier. The normal operation is divided into three phases based on the number of involved transformer windings.

*Phase 1:* The bridge being connected to winding  $a_2x_2$  is working. The output voltage can be regulated from 0 to  $1/2u_d(t)$  by controlling  $VT_5/VT_6$ .  $VT_1 \sim VT_4$  are not triggered in this phase.

*M1( $t_1 \sim t_2$ ):*  $VT_5$  is cutoff by the reverse voltage at  $t_1$ . The current path in M1 is  $VD_2 \rightarrow VD_1 \rightarrow VD_4 \rightarrow VD_3 \rightarrow \text{Load}$ .  $u_1(t) = 0$  till  $VT_6$  is turned ON at  $t_2$ . The forward voltage drop of  $VT_x$  and  $VD_x$  are negligible, and  $i_2(t)$  is ignored because the resistances of 75R and 76R are big enough. The simplified equivalent-circuit diagram in M1 is shown in Fig. 3(a), where  $L_2$  is the inductance value of the traction motor reactor;  $I_1$  is

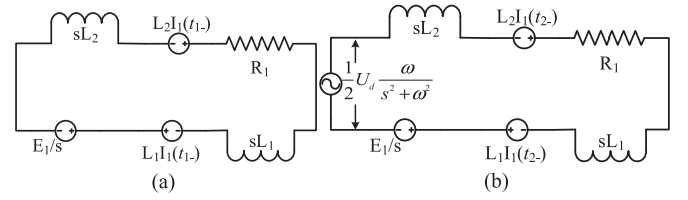


Fig. 3. Simplified equivalent-circuit diagram in M1 and M2. (a) Equivalent circuit in M1. (b) Equivalent circuit in M2.

the output current;  $R_1$ ,  $L_1$ , and  $E_1$  are equivalent resistance, inductance, and back EMF of the traction motor, respectively. Kirchhoff's law-based loop equation for M1 is

$$0 \cong sL_2I_1 - L_2I_1(t_{1-}) + R_1I_1 + sL_1I_1 - L_1I_1(t_{1-}) + E_1/s. \quad (1)$$

By solving the loop equation (1),  $i_1(t)$  can be obtained as

$$i_1(t) = B_1e^{-B_2t} - B_3\varepsilon(t) \quad (2)$$

where  $B_1 = I_1(t_{1-}) + \frac{E_1}{B_2}$ ,  $B_2 = \frac{R_1}{L_1+L_2}$ ,  $B_3 = \frac{E_1}{B_2}$ .

*M2( $t_2 \sim t_3$ ):*  $VT_6$  is turned ON at  $t_2$ . The current goes through the path:  $a_2 \rightarrow VD_3 \rightarrow \text{Load} \rightarrow VD_2 \rightarrow VD_1 \rightarrow VT_6 \rightarrow x_2$ . The rectifier goes into M3 when  $u_d(t)$  crosses zero at  $t_3$ .  $u_1(t) = 1/2u_d(t)$ . The simplified equivalent circuit in M2 is shown in Fig. 3(b).  $i_1(t)$  in M2 can be obtained as

$$i_1(t) = A_1e^{-A_2t} + A_2\sqrt{A_3} \cos\left(\omega t + \tan^{-1}\frac{B_2}{\omega}\right) - \frac{E_1}{R_1}(1 - A_4e^{-B_2t}) \quad (3)$$

where

$$A_1 = \frac{A_5\omega(L_1+L_2)u_d}{[\omega^2(L_1+L_2)^2+R_1^2]}, \quad A_2 = \frac{A_5u_d\sqrt{\omega^2(L_1+L_2)^2+R_1^2}}{[\omega^2(L_1+L_2)^2-R_1^2]},$$

$$A_3 = \tan^{-1}\frac{B_2}{\omega}, \quad A_4 = \frac{E_1 - R_1I_1(t_{1-})}{E_1}, \quad A_5 = 1/2.$$

*M3( $t_3 \sim t_4$ ):* M3 is similar to M1.  $u_1(t) = 0$  in this mode.  $VT_5$  is turned ON at  $t_4$ .

*M4( $t_4 \sim t_5$ ):*  $VT_5$  is turned ON at  $t_4$  and  $t_4$  is chosen according to the load. The current path in M4 is  $x_2 \rightarrow VT_5 \rightarrow \text{Load} \rightarrow VD_2 \rightarrow VD_1 \rightarrow VD_4 \rightarrow a_2$ .  $u_1(t)$  and  $i_1(t)$  in M4 obey same rules as in M2 but with different initials. Then, the rectifier goes into next working cycle after  $VT_5$  is turned OFF at  $t_5$ .

The rectifier operation is turned into the second phase when  $u_1(t)$  is increasing over  $1/2u_d(t)$ , the bridge connected to winding  $a_1b_1$  starts to operate. In the second phase,  $VT_5$  and  $VT_6$  are fully triggered,  $VT_3$  and  $VT_4$  are not triggered.  $VT_1$  and  $VT_2$  are controlled to adjust  $u_1(t)$ .  $u_1(t)$  will exceed  $3/4u_d(t)$  in the third phase, the bridge connected to winding  $b_1x_1$  starts to work,  $VT_1$ ,  $VT_2$ ,  $VT_5$ , and  $VT_6$  are fully triggered in this phase. All operations in the second phase and the third phase are much alike those in the first phase. They also can be subdivided into four modes, respectively. Parameters and behavior of each mode are given in Table II.

TABLE II  
PARAMETERS AND BEHAVIOR OF THE RECTIFIER IN PHASE 2 AND PHASE 3

Mode	Phase	$u_1(t)$	$i_1(t)$	Control of VT <sub>1</sub> – VT <sub>6</sub>
M5 : $t_6 \sim t_7$	2	$1/2u_d(t)$	Similar to (2) with different initial value	VT <sub>1</sub> /VT <sub>2</sub> are triggered according to load
M6 : $t_7 \sim t_8$	2	$3/4u_d(t)$	Similar to (3) with $A_5 = 3/4$	VT <sub>3</sub> /VT <sub>4</sub> are not triggered VT <sub>5</sub> /VT <sub>6</sub> are fully triggered
M7 : $t_8 \sim t_9$	2	$1/2u_d(t)$	Similar to (2) with different initial value	triggered
M8 : $t_9 \sim t_{10}$	2	$3/4u_d(t)$	Similar to (3) with $AA_5 = 3/4$	
M9 : $t_{11} \sim t_{12}$	3	$3/4u_d(t)$	Similar to (2) with different initial value	VT <sub>1</sub> /VT <sub>2</sub> are fully triggered
M10 : $t_{12} \sim t_{13}$	3	$u_d(t)$	Similar to (3) with $A_5 = 1$	VT <sub>3</sub> /VT <sub>4</sub> are triggered according to load
M11 : $t_{13} \sim t_{14}$	3	$3/4u_d(t)$	Similar to (2) with different initial value	VT <sub>5</sub> /VT <sub>6</sub> are fully triggered
M12 : $t_{14} \sim t_{15}$	3	$u_d(t)$	Similar to (3) with $A_5 = 1$	

TABLE III  
ALL POSSIBLE RECTIFYING AND FREEWHEELING PATH FOR THE RECTIFIER

x	Connected Winding	Winding Voltage	Rectifying path	Corresponding possible freewheeling path
1	$a_1 b_1$	$1/4u_d(t)$	VT <sub>1</sub> /VD <sub>2</sub>	VD <sub>3</sub> /VD <sub>4</sub> , VT <sub>5</sub> /VD <sub>4</sub> VT <sub>6</sub> /VD <sub>3</sub> , VT <sub>5</sub> /VT <sub>6</sub>
2	$a_1 b_1$	$1/4u_d(t)$	VT <sub>2</sub> /VD <sub>1</sub>	VD <sub>3</sub> /VD <sub>4</sub> , VT <sub>5</sub> /VD <sub>4</sub> VT <sub>6</sub> /VD <sub>3</sub> , VT <sub>5</sub> /VT <sub>6</sub>
3	$b_1 x_1$	$1/4u_d(t)$	VT <sub>1</sub> /VT <sub>4</sub>	VD <sub>3</sub> /VD <sub>4</sub> , VT <sub>5</sub> /VD <sub>4</sub> VT <sub>6</sub> /VD <sub>3</sub> , VT <sub>5</sub> /VT <sub>6</sub>
4	$b_1 x_1$	$1/4u_d(t)$	VT <sub>2</sub> /VT <sub>3</sub>	VD <sub>3</sub> /VD <sub>4</sub> , VT <sub>5</sub> /VD <sub>4</sub> VT <sub>6</sub> /VD <sub>3</sub> , VT <sub>5</sub> /VT <sub>6</sub>
5	$a_1 x_1$	$1/2u_d(t)$	VT <sub>3</sub> /VD <sub>2</sub>	VD <sub>3</sub> /VD <sub>4</sub> , VT <sub>5</sub> /VD <sub>4</sub> VT <sub>6</sub> /VD <sub>3</sub> , VT <sub>5</sub> /VT <sub>6</sub>
6	$a_1 x_1$	$1/2u_d(t)$	VT <sub>4</sub> /VD <sub>1</sub>	VD <sub>3</sub> /VD <sub>4</sub> , VT <sub>5</sub> /VD <sub>4</sub> VT <sub>6</sub> /VD <sub>3</sub> , VT <sub>5</sub> /VT <sub>6</sub>
7	$a_2 x_2$	$1/2u_d(t)$	VT <sub>5</sub> /VD <sub>4</sub>	VD <sub>1</sub> /VD <sub>2</sub> , VT <sub>1</sub> /VD <sub>2</sub> , VT <sub>2</sub> /VD <sub>1</sub> VT <sub>3</sub> /VD <sub>2</sub> , VT <sub>4</sub> /VD <sub>1</sub> , VT <sub>1</sub> /VT <sub>4</sub> VT <sub>2</sub> /VT <sub>3</sub> , VT <sub>1</sub> /VT <sub>2</sub> , VT <sub>3</sub> /VT <sub>4</sub>
8	$a_2 x_2$	$1/2u_d(t)$	VT <sub>6</sub> /VD <sub>3</sub>	VD <sub>1</sub> /VD <sub>2</sub> , VT <sub>1</sub> /VD <sub>2</sub> , VT <sub>2</sub> /VD <sub>1</sub> VT <sub>3</sub> /VD <sub>2</sub> , VT <sub>4</sub> /VD <sub>1</sub> , VT <sub>1</sub> /VT <sub>4</sub> VT <sub>2</sub> /VT <sub>3</sub> , VT <sub>1</sub> /VT <sub>2</sub> , VT <sub>3</sub> /VT <sub>4</sub>

### B. Analysis of the Faulty Operation

Based on the analysis above, the essence of the bridge rectifier working mechanism is that corresponding switches are turned ON to apply the input voltage directly on the load when the load current needs to be increased. On the perspective of each transformer winding, if all switches on the rectifying path are turned ON and there is at least one freewheeling path conducting, the voltage on that transformer winding is applied directly to the load. Take winding  $a_1 b_1$  as an example, if VT<sub>1</sub> and VD<sub>2</sub> are turned ON, and at least one of the four possible freewheeling paths in Table III is conducting, the voltage  $1/4u_d(t)$  provided by winding  $a_1 b_1$  is added to the output voltage  $u_1(t)$  and applied on the load. Similarly, other transformer windings obey the same rule. All possible rectifying and freewheeling path of this rectifier are listed in Table III. Based on the analysis above, the voltage transfer function is proposed as

follows:

$$u_1(t) = \frac{1}{2}|u_d(t)| \times \sum_{x=5}^8 f_{dx}(t) \times f_{fx}(t) \times SIGN_x(t) + \frac{1}{4}|u_d(t)| \times \sum_{x=1}^4 f_{dx}(t) \times f_{fx}(t) \times SIGN_x(t) \quad (4)$$

where  $f_{dx}(t)$  is the state function of the rectifying path.  $f_{fx}(t)$  is the state function of corresponding freewheeling path to the rectifying path.  $SIGN(t)$  is the function that describes the orientation of the corresponding rectified voltage.

Define  $f_{VT_x}(t)$  and  $f_{VD_y}(t)$  to represent on and off state of each switches in the rectifier

$$f_{VT_x}(t) = \begin{cases} 1, & \text{VT}_x \text{ is turned ON} \\ 0, & \text{VT}_x \text{ is turned OFF} \end{cases} \quad x = 1, 2, 3, 4, 5, 6$$

$$f_{VD_y}(t) = \begin{cases} 1, & \text{VD}_y \text{ is turned ON} \\ 0, & \text{VD}_y \text{ is turned OFF} \end{cases} \quad y = 1, 2, 3, 4. \quad (5)$$

According Table III, the definition of the rectifying path state function  $f_{dx}(t)$  and the freewheeling path state function  $f_{fx}(t)$  are proposed as follows:

$$f_{dx}(t) = \begin{cases} [f_{VT_1}(t) \& f_{VD_2}(t)], & x = 1 \\ [f_{VT_2}(t) \& f_{VD_1}(t)], & x = 2 \\ [f_{VT_1}(t) \& f_{VT_4}(t)], & x = 3 \\ [f_{VT_2}(t) \& f_{VT_3}(t)], & x = 4 \\ [f_{VT_3}(t) \& f_{VD_2}(t)], & x = 5 \\ [f_{VT_4}(t) \& f_{VD_1}(t)], & x = 6 \\ [f_{VT_5}(t) \& f_{VD_4}(t)], & x = 7 \\ [f_{VT_6}(t) \& f_{VD_3}(t)], & x = 8 \end{cases} \quad (6)$$

$$f_{fx}(t) = \begin{cases} [f_{VD_3}(t) \& f_{VD_4}(t)] || [f_{VT_5}(t) \& f_{VD_4}(t)] || [f_{VT_6}(t) \& f_{VD_3}(t)] \\ || [f_{VT_5}(t) \& f_{VT_6}(t)] & x = 1, 2, 3, 4, 5, 6 \\ [f_{VD_1}(t) \& f_{VD_2}(t)] || [f_{VT_1}(t) \& f_{VT_2}(t)] || [f_{VT_3}(t) \& f_{VT_4}(t)] \\ || [f_{VT_1}(t) \& f_{VD_2}(t)] || [f_{VT_2}(t) \& f_{VD_1}(t)] || [f_{VT_3}(t) \& f_{VD_2}(t)] \\ || [f_{VT_4}(t) \& f_{VD_1}(t)] || [f_{VT_1}(t) \& f_{VT_4}(t)] || [f_{VT_2}(t) \& f_{VT_3}(t)] & x = 7, 8 \end{cases} \quad (7)$$

Take direction of  $u_1(t)$  in Fig. 1 as the reference,  $SIGN_x(t)$  is defined below to describe the orientation of the rectified voltage

$$SIGN_x(t) = \begin{cases} 1, & \text{same direction with } u_1(t) \\ -1, & \text{different direction with } u_1(t) \\ 0, & \text{rectified voltage equals 0} \end{cases} \quad (8)$$

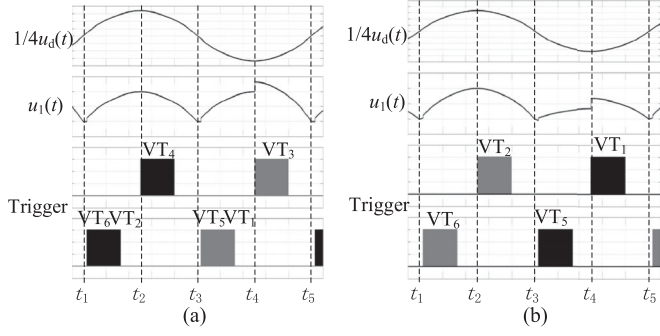


Fig. 4. Waveforms of open-circuit fault under new steady state. (a)  $VT_4$  open-circuit fault in phase 3. (b)  $VD_2$  open-circuit fault in phase 2.

Take  $VT_4$  open-circuit fault as an example, assume that the rectifier is working in Phase 3, and the new steady state of the rectifier is reached. One rectifier working cycle is divided into four stages, and the simulation waveform is shown in Fig. 4:

*Stage 1* ( $t_1 \sim t_2$ ): The rectifier is working in Phase 3 and  $u_d(t)$  is on its positive half cycle. Based on the analysis in Section III-A, we can get that  $VT_2/VT_6/VD_1/VD_3$  are turned ON and  $VT_1/VT_3/VT_4/VT_5/VD_2/VD_4$  are cut off. By Eq.(5)–(8), we have

$$f_{dx}(t) = \begin{cases} 0, & x = 1 \\ 1, & x = 2 \\ 0, & x = 3 \\ 0, & x = 4 \\ 0, & x = 5 \\ 0, & x = 6 \\ 0, & x = 7 \\ 1, & x = 8 \end{cases}; \quad SIGN_x(t) = \begin{cases} 0, & x = 1 \\ 1, & x = 2 \\ 0, & x = 3 \\ 0, & x = 4 \\ 0, & x = 5 \\ 0, & x = 6 \\ 0, & x = 7 \\ 1, & x = 8 \end{cases};$$

$$f_{ix}(t) = \begin{cases} 1, & x = 1 \\ 1, & x = 2 \\ 1, & x = 3 \\ 1, & x = 4 \\ 1, & x = 5 \\ 1, & x = 6 \\ 1, & x = 7 \\ 1, & x = 8 \end{cases}; \quad f_{VT_x}(t) = \begin{cases} 0, & x = 1 \\ 1, & x = 2 \\ 0, & x = 3 \\ 0, & x = 4 \\ 0, & x = 5 \\ 0, & x = 6 \end{cases};$$

$$f_{VD_y}(t) = \begin{cases} 1, & y = 1 \\ 0, & y = 2 \\ 1, & y = 3 \\ 0, & y = 4 \end{cases}.$$

Applying the result in (4), we have  $u_1(t) = 3/4u_d(t)$ .

*Stage 2* ( $t_2 \sim t_3$ ): Because  $VT_4$  is an open circuit and cannot be turned ON, the state of both rectifying and freewheeling paths are same as in Stage 1, thus,  $u_1(t) = 3/4u_d(t)$ .

*Stage 3* ( $t_3 \sim t_4$ ):  $u_d(t)$  goes into its negative half cycle; according to Section III-A,  $VT_1/VT_5/VD_2/VD_4$  are turned

ON and  $VT_2/VT_3/VT_4/VT_6/VD_1/VD_3$  are cutoff. Thus

$$f_{dx}(t) = \begin{cases} 1, & x = 1 \\ 0, & x = 2 \\ 0, & x = 3 \\ 0, & x = 4 \\ 0, & x = 5 \\ 0, & x = 6 \\ 1, & x = 7 \\ 0, & x = 8 \end{cases}; \quad SIGN_x(t) = \begin{cases} 1, & x = 1 \\ 0, & x = 2 \\ 0, & x = 3 \\ 0, & x = 4 \\ 0, & x = 5 \\ 0, & x = 6 \\ 1, & x = 7 \\ 0, & x = 8 \end{cases};$$

$$f_{ix}(t) = \begin{cases} 1, & x = 1 \\ 1, & x = 2 \\ 1, & x = 3 \\ 1, & x = 4 \\ 1, & x = 5 \\ 1, & x = 6 \\ 1, & x = 7 \\ 1, & x = 8 \end{cases}; \quad f_{VT_x}(t) = \begin{cases} 1, & x = 1 \\ 0, & x = 2 \\ 0, & x = 3 \\ 0, & x = 4 \\ 1, & x = 5 \\ 0, & x = 6 \end{cases};$$

$$f_{VD_y}(t) = \begin{cases} 0, & y = 1 \\ 1, & y = 2 \\ 0, & y = 3 \\ 1, & y = 4 \end{cases}.$$

So, we can get  $u_1(t) = 3/4u_d(t)$  from (4).

*Stage 4* ( $t_4 \sim t_5$ ):  $VT_3$  is turned ON and caused  $VT_1$  cutting off. Thus

$$f_{dx}(t) = \begin{cases} 0, & x = 1 \\ 0, & x = 2 \\ 0, & x = 3 \\ 0, & x = 4 \\ 1, & x = 5 \\ 0, & x = 6 \\ 1, & x = 7 \\ 0, & x = 8 \end{cases}; \quad SIGN_x(t) = \begin{cases} 0, & x = 1 \\ 0, & x = 2 \\ 0, & x = 3 \\ 0, & x = 4 \\ 1, & x = 5 \\ 0, & x = 6 \\ 1, & x = 7 \\ 0, & x = 8 \end{cases};$$

$$f_{ix}(t) = \begin{cases} 1, & x = 1 \\ 1, & x = 2 \\ 1, & x = 3 \\ 1, & x = 4 \\ 1, & x = 5 \\ 1, & x = 6 \\ 1, & x = 7 \\ 1, & x = 8 \end{cases}; \quad f_{VT_x}(t) = \begin{cases} 0, & x = 1 \\ 0, & x = 2 \\ 1, & x = 3 \\ 0, & x = 4 \\ 1, & x = 5 \\ 0, & x = 6 \end{cases};$$

$$f_{VD_y}(t) = \begin{cases} 0, & y = 1 \\ 1, & y = 2 \\ 0, & y = 3 \\ 1, & y = 4 \end{cases}.$$

By calculating (4),  $u_1(t) = u_d(t)$ . The simulation waveform is shown in Fig. 4(a).

There are two special situations to be discussed here. The anode voltage of  $VT_2$  is increased by  $1/4u_d(t)$  due to the

conduction of  $VT_4$ , so  $VT_2$  is cutoff by enduring a reverse voltage. The conduction of  $VT_3$  will cut off  $VT_1$  by the same reason, i.e.,  $f_{VT_4}(t) = 1$  and  $f_{VT_1}(t) = 1$  will lead to  $f_{VT_1}(t) = 0$  and  $f_{VT_3}(t) = 0$ , respectively. Furthermore,  $VD_2$  ( $VD_1$ ) open-circuit fault will introduce a sustain forward voltage on  $VT_2$ / $VT_4$  ( $VT_1$ / $VT_3$ ), which means if  $VD_2$  ( $VD_1$ ) open-circuit fault happened in Phase 3,  $VT_4$  ( $VT_3$ ) is turned ON and  $VT_2$  ( $VT_1$ ) is bypassed all the time in the new steady state.

Take  $VD_2$  open-circuit fault as another example, assume that the rectifier is working in Phase 2, and the new steady state of the rectifier is reached.

*Stage 1* ( $t_1 \sim t_2$ ): The rectifier is working in Phase 2 and  $u_d(t)$  is at its positive half cycle. Though  $VT_2$  is not triggered,  $VD_2$  open-circuit fault will cause the nonstop conduction of  $VT_2$ . Thus, the switches states are the same as those in  $VT_4$  open-circuit fault Stage 1, which means  $u_1(t) = 3/4u_d(t)$ .

*Stage 2* ( $t_2 \sim t_3$ ):  $VT_2$  is triggered, but all the switches states stay unchanged, so  $u_1(t) = 3/4u_d(t)$ .

*Stage 3* ( $t_3 \sim t_4$ ):  $u_d(t)$  goes into the negative half cycle,  $VT_2$  continues conducting and  $VT_1$  is not triggered. So,  $VT_2$ / $VT_5$ / $VD_1$ / $VD_4$  are turned ON and  $VT_1$ / $VT_3$ / $VT_4$ / $VT_6$ / $VD_2$ / $VD_3$  are turned OFF. Notice that,  $VT_2$ / $VD_1$  is conducting in the negative half cycle of  $u_d(t)$ , which makes the voltage polarity of winding  $a_1b_1$  opposite to the output voltage  $u_1(t)$ , i.e.,  $SIGN_2(t) = -1$ . Thus

$$f_{dx}(t) = \begin{cases} 0, & x = 1 \\ 1, & x = 2 \\ 0, & x = 3 \\ 0, & x = 4 \\ 0, & x = 5 \\ 0, & x = 6 \\ 1, & x = 7 \\ 0, & x = 8 \end{cases}; \quad SIGN_x(t) = \begin{cases} 0, & x = 1 \\ -1, & x = 2 \\ 0, & x = 3 \\ 0, & x = 4 \\ 0, & x = 5 \\ 0, & x = 6 \\ 1, & x = 7 \\ 0, & x = 8 \end{cases};$$

$$f_{fx}(t) = \begin{cases} 1, & x = 1 \\ 1, & x = 2 \\ 1, & x = 3 \\ 1, & x = 4 \\ 1, & x = 5 \\ 1, & x = 6 \\ 1, & x = 7 \\ 1, & x = 8 \end{cases}; \quad f_{VT_x}(t) = \begin{cases} 0, & x = 1 \\ 1, & x = 2 \\ 0, & x = 3 \\ 0, & x = 4 \\ 0, & x = 5 \\ 1, & x = 6 \\ 0, & x = 7 \\ 0, & x = 8 \end{cases};$$

$$f_{VD_y}(t) = \begin{cases} 1, & y = 1 \\ 0, & y = 2 \\ 0, & y = 3 \\ 1, & y = 4 \end{cases}.$$

Applying the result in (4), we get  $u_1(t) = 1/4u_d(t)$ .

*Stage 4* ( $t_4 \sim t_5$ ):  $VT_1$  is triggered and  $VD_1$  is cutoff, thus

$$f_{dx}(t) = \begin{cases} 0, & x = 1 \\ 0, & x = 2 \\ 0, & x = 3 \\ 0, & x = 4 \\ 0, & x = 5 \\ 0, & x = 6 \\ 1, & x = 7 \\ 0, & x = 8 \end{cases}; \quad SIGN_x(t) = \begin{cases} 0, & x = 1 \\ 0, & x = 2 \\ 0, & x = 3 \\ 0, & x = 4 \\ 0, & x = 5 \\ 0, & x = 6 \\ 1, & x = 7 \\ 0, & x = 8 \end{cases};$$

$$f_{fx}(t) = \begin{cases} 1, & x = 1 \\ 1, & x = 2 \\ 1, & x = 3 \\ 1, & x = 4 \\ 1, & x = 5 \\ 1, & x = 6 \\ 1, & x = 7 \\ 1, & x = 8 \end{cases}; \quad f_{VT_x}(t) = \begin{cases} 1, & x = 1 \\ 1, & x = 2 \\ 0, & x = 3 \\ 0, & x = 4 \\ 1, & x = 5 \\ 0, & x = 6 \end{cases};$$

$$f_{VD_y}(t) = \begin{cases} 0, & y = 1 \\ 0, & y = 2 \\ 0, & y = 3 \\ 1, & y = 4 \end{cases}$$

and  $u_1(t) = u_d(t)$ . The result waveform is shown in Fig. 4(b).

The output voltage  $u_1(t)$  of other open-circuit faults under different phases can be obtained by the same reasoning, which is shown in Table IV. Only one of the two switches in each leg are mentioned in Table IV, because the faulty output voltages are similar for upper or lower switch open-circuit fault on the same leg, the only difference is the displacement angle.

### C. Fault Diagnosis Based on the Voltage Transfer Function

*1) Method Design:* The phase-shift angle adjustment range of a practical rectifier is usually limited from  $5^\circ$  to  $175^\circ$  due to the actual application conditions, such as the threshold and time delay of the acquisition circuit, as well as the limitation of thyristors and so on[24]. These considerations are taken into account by the following analysis. It is easy to find out that the relationship between  $u_1(t)$  and  $u_d(t)$  is piecewise-linearity in all three phases under both normal and faulty states.  $u_1(t)$  could be shifted in amplitude to extract fault feature. Therefore, the fault characteristic equation is proposed as follows:

$$\begin{cases} zc1(t) = u_1(t) - \frac{3}{4}|u_d(t)| \\ zc2(t) = u_1(t) - \frac{1}{2}|u_d(t)| \\ zc3(t) = u_1(t) - \frac{1}{4}|u_d(t)| \end{cases} \quad (9)$$

TABLE IV  
CONVERTER STATES UNDER OPEN-CIRCUIT FAULT

Period	$u_1(t)$	Faulty switch	Phase	Period	$u_1(t)$	Faulty switch	Phase
$t_1 \sim t_2$	$3/4 u_d(t) $	VT <sub>4</sub>	3	$t_1 \sim t_2$	0	VT <sub>6</sub>	2
$t_2 \sim t_3$	$3/4 u_d(t) $	VT <sub>4</sub>	3	$t_2 \sim t_3$	$1/4 u_d(t) $	VT <sub>6</sub>	2
$t_3 \sim t_4$	$3/4 u_d(t) $	VT <sub>4</sub>	3	$t_3 \sim t_4$	$1/2 u_d(t) $	VT <sub>6</sub>	2
$t_4 \sim t_5$	$ u_d(t) $	VT <sub>4</sub>	3	$t_4 \sim t_5$	$3/4 u_d(t) $	VT <sub>6</sub>	2
$t_1 \sim t_2$	$3/4 u_d(t) $	VT <sub>1</sub>	3	$t_1 \sim t_2$	$3/4 u_d(t) $	VD <sub>2</sub>	2
$t_2 \sim t_3$	$ u_d(t) $	VT <sub>1</sub>	3	$t_2 \sim t_3$	$3/4 u_d(t) $	VD <sub>2</sub>	2
$t_3 \sim t_4$	$1/2 u_d(t) $	VT <sub>1</sub>	3	$t_3 \sim t_4$	$1/4 u_d(t) $	VD <sub>2</sub>	2
$t_4 \sim t_5$	$ u_d(t) $	VT <sub>1</sub>	3	$t_4 \sim t_5$	$1/2 u_d(t) $	VD <sub>2</sub>	2
$t_1 \sim t_2$	$ u_d(t) $	VD <sub>2</sub>	3	$t_1 \sim t_2$	$1/2 u_d(t) $	VD <sub>4</sub>	2
$t_2 \sim t_3$	$ u_d(t) $	VD <sub>2</sub>	3	$t_2 \sim t_3$	$3/4 u_d(t) $	VD <sub>4</sub>	2
$t_3 \sim t_4$	$1/4 u_d(t) $	VD <sub>2</sub>	3	$t_3 \sim t_4$	0	VD <sub>4</sub>	2
$t_4 \sim t_5$	$1/2 u_d(t) $	VD <sub>2</sub>	3	$t_4 \sim t_5$	$1/4 u_d(t) $	VD <sub>4</sub>	2
$t_1 \sim t_2$	$1/4 u_d(t) $	VT <sub>6</sub>	3	$t_1 \sim t_2$	0	VT <sub>6</sub>	1
$t_2 \sim t_3$	$1/2 u_d(t) $	VT <sub>6</sub>	3	$t_2 \sim t_3$	0	VT <sub>6</sub>	1
$t_3 \sim t_4$	$3/4 u_d(t) $	VT <sub>6</sub>	3	$t_3 \sim t_4$	0	VT <sub>6</sub>	1
$t_4 \sim t_5$	$ u_d(t) $	VT <sub>6</sub>	3	$t_4 \sim t_5$	$1/2 u_d(t) $	VT <sub>6</sub>	1
$t_1 \sim t_2$	$3/4 u_d(t) $	VD <sub>4</sub>	3	$t_1 \sim t_2$	0	VD <sub>4</sub>	1
$t_2 \sim t_3$	$ u_d(t) $	VD <sub>4</sub>	3	$t_2 \sim t_3$	$1/2 u_d(t) $	VD <sub>4</sub>	1
$t_3 \sim t_4$	$1/4 u_d(t) $	VD <sub>4</sub>	3	$t_3 \sim t_4$	$-1/2 u_d(t) $	VD <sub>4</sub>	1
$t_4 \sim t_5$	$1/2 u_d(t) $	VD <sub>4</sub>	3	$t_4 \sim t_5$	0	VD <sub>4</sub>	1
$t_1 \sim t_2$	$1/2 u_d(t) $	VT <sub>1</sub>	2	$t_1 \sim t_2$	0	VD <sub>2</sub>	1
$t_2 \sim t_3$	$3/4 u_d(t) $	VT <sub>1</sub>	2	$t_2 \sim t_3$	0	VD <sub>2</sub>	1
$t_3 \sim t_4$	$1/2 u_d(t) $	VT <sub>1</sub>	2	$t_3 \sim t_4$	0	VD <sub>2</sub>	1
$t_4 \sim t_5$	$1/2 u_d(t) $	VT <sub>1</sub>	2	$t_4 \sim t_5$	0	VD <sub>2</sub>	1

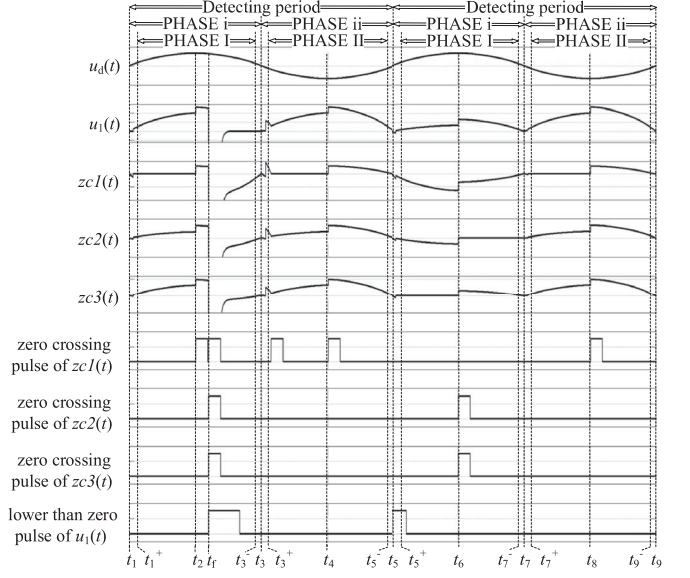


Fig. 5. Sequence diagram for VD<sub>3</sub> open-circuit fault analysis in phase 3.

Define  $t_1 \sim t_5$  as in

$$\left\{ \begin{array}{l} t_1, t_5 : u_d(t) = 0, u_d(t^+) > 0, u_d(t^-) < 0; \\ t_3 : u_d(t) = 0, u_d(t^+) < 0, u_d(t^-) > 0; \\ t_2, t_4 : f_{dx}(t^-) \neq f_{dx}(t^+); \\ t_1 < t_2 < t_3 < t_4 < t_5; \\ t^+ - t \geq 0.28 \text{ ms}; \\ t - t^- \geq 0.28 \text{ ms}; \end{array} \right. \quad (10)$$

A working cycle is split into four periods:  $t_1^+ \sim t_2$ ,  $t_2 \sim t_3^-$ ,  $t_3^+ \sim t_4$ , and  $t_4 \sim t_5^-$ . Define zero-crossing as a function value becoming more than zero from less than or equal to zero and vice versa. Then, a fault diagnosis function is proposed to calculate zero-crossing times of (9), and another fault diagnosis function is proposed to calculate times of  $u_1(t)$  less than zero

$$ZCx_y(m) = \begin{cases} ZCx_y(m) + 1 & zcx(t) \text{ Zero - Crossing} \\ ZCx_y(m) & \text{Other situation} \end{cases}$$

$$ZC4_z(m) = \begin{cases} ZC4_z(m) + 1 & u_1(t) < 0 \\ ZC4_z(m) & u_1(t) \geq 0 \end{cases} \quad (11)$$

where  $x = (1, 2, 3)$ ;  $y = (p, n)$ ,  $y = p$  stands for  $t_1^+ \sim t_3^-$  (PHASE I),  $y = n$  stands for  $t_3^+ \sim t_5^-$  (PHASE II);  $z = (p, n)$ ,  $z = p$  stands for  $t_1 \sim t_3$  (PHASE i),  $z = n$  stands for  $t_3 \sim t_5$  (PHASE ii);  $ZCx_y(m)$  and  $ZC4_z(m)$  are calculated for every half-cycle of  $u_d(t)$ , and  $m$  is a natural number indicating the computing times.

The zero-crossing times vector and its transfer vector are designed as shown in (12) and (13), the fault vector operator is

proposed as shown in (14)

$$Z(m) = [ZC1_p(m) \ ZC2_p(m) \ ZC3_p(m) \ ZC4_p(m) \\ ZC1_n(m) \ ZC2_n(m) \ ZC3_n(m) \ ZC4_n(m)] \quad (12)$$

$$b = [128 \ 64 \ 32 \ 16 \ 8 \ 4 \ 2 \ 1]^T \quad (13)$$

$$C(m) = Z(m) \bullet b. \quad (14)$$

Take VD<sub>3</sub> open-circuit fault in phase 3 as an example to demonstrate the fault diagnosis process. According to (10), one detecting period in Fig. 5 is divided into PHASE I, PHASE II, PHASE i, and PHASE ii. In PHASE I, the zero-crossing in  $t_1 \sim t_1^+$  period is eliminated because  $t_1^+ - t_1 \geq 0.28$  ms.  $zc1(t)$  cross zero at  $t_2$  because VT<sub>6</sub> is triggered. Then, VD<sub>3</sub> is an open circuit at  $t_f$ , which makes  $zc1(t)$ ,  $zc2(t)$ , and  $zc3(t)$  drop to below zero. In PHASE I,  $zc1(t)$  crosses zero twice, while  $zc2(t)$  and  $zc3(t)$  cross zero once. According to (11),  $ZCx_y(m-1)$  are calculated as follows:

$$\begin{cases} ZC1_p(m-1) = 2 \\ ZC2_p(m-1) = 1 \\ ZC3_p(m-1) = 1 \end{cases}, \begin{cases} ZC1_n(m-1) = 2 \\ ZC2_n(m-1) = 0 \\ ZC3_n(m-1) = 0 \end{cases}.$$

In PHASE i,  $u_1(t) < 0$  at  $t_f$  due to VD<sub>3</sub> open-circuit fault, and consequently, we have

$$ZC4_p(m-1) = 1, \ ZC4_n(m-1) = 0.$$

Thus, by applying  $ZCx_y(m-1)$  and  $ZC4_z(m-1)$  into (12)–(14),  $Z(m-1)$  and  $C(m-1)$  is acquired as follows and the fault is detected

$$Z(m-1) = [2 \ 1 \ 1 \ 1 \ 2 \ 0 \ 0 \ 0], \ C(m-1) = 384(D) \\ = 110000000(B).$$

TABLE V  
STATE VECTOR TABLE

Faulty switch	$C(m)$	Phase	Faulty switch	$C(m)$	Phase
Normal	10001000	3	VD <sub>3</sub>	00111100	2
VD <sub>1</sub>	01110000	3	VD <sub>4</sub>	11000011	2
VD <sub>2</sub>	00000111	3	VT <sub>1</sub>	11000000	2
VD <sub>3</sub>	01111000	3	VT <sub>2</sub>	00001100	2
VD <sub>4</sub>	10000111	3	VT <sub>5</sub>	11000010	2
VT <sub>1</sub>	10001100	3	VT <sub>6</sub>	00101100	2
VT <sub>2</sub>	11001000	3	Normal	01100110	1
VT <sub>3</sub>	10000000	3	VD <sub>3</sub>	00011111	1
VT <sub>4</sub>	00001000	3	VD <sub>4</sub>	11110001	1
VT <sub>5</sub>	10000110	3	VT <sub>5</sub>	01110000	1
VT <sub>6</sub>	01101000	3	VT <sub>6</sub>	00000111	1
Normal	11001100	2	VD <sub>1</sub>	00000000	1
VD <sub>1</sub>	01110000	2	VD <sub>2</sub>	00000000	1
VD <sub>2</sub>	00000111	2			

By applying same reasoning in the next detecting period, we have

$$\begin{cases} ZC1_p(m) = 0 \\ ZC2_p(m) = 1 \\ ZC3_p(m) = 1 \end{cases}, \begin{cases} ZC1_n(m) = 1 \\ ZC2_n(m) = 0 \\ ZC3_n(m) = 0 \end{cases}$$

Notice that, under VD<sub>3</sub> open-circuit fault, the voltage on VT<sub>5</sub> is always positive, and VT<sub>5</sub> cannot be turned OFF. Thus, during  $t_5 \sim t_5^+$ , VD<sub>1</sub>, VD<sub>2</sub>, VD<sub>4</sub>, and VT<sub>5</sub> are involved in current conducting until VT<sub>6</sub> and VT<sub>2</sub> are turned ON at  $t_5^+$ .  $u_1(t)$  is equal to  $-1/2u_d(t)$  in this time interval. After VT<sub>6</sub> and VT<sub>2</sub> are turned ON, the current goes through VD<sub>1</sub>, VT<sub>2</sub>, VT<sub>5</sub>, and VT<sub>6</sub>,  $u_1(t)$  has stepped from  $-1/2u_d(t)$  to  $1/4u_d(t)$  and kept positive since then, which makes  $ZC4_p(m) = 1$  in PHASE i. In the following time interval  $t_7 \sim t_9$ ,  $u_d(t)$  is always negative. First, VT<sub>6</sub> and VT<sub>2</sub> are turned OFF, the current is freewheeling by VD<sub>1</sub>, VD<sub>2</sub>, VD<sub>4</sub>, and VT<sub>5</sub>,  $u_1(t)$  is equal to  $-1/2u_d(t)$  until VT<sub>1</sub> is turned ON at  $t_7^+$ . Then,  $u_1(t)$  equals to  $-3/4u_d(t)$  and  $-u_d(t)$  at  $t_7^+$  and  $t_8$ , respectively.  $ZC4_n(m) = 0$  in this period, therefore,

$$C(m) = 120(D) = 01111000(B).$$

VD<sub>3</sub> open circuit is located. All other state codes are calculated in a similar way and shown in Table V. Notice that, because the faulty phenomenon of VD<sub>1</sub> and VD<sub>2</sub> open-circuit fault in Phase 1 are identical to each other, there  $C(m)$  are the same. So, if VD<sub>1</sub> or VD<sub>2</sub> open-circuit fault happens in Phase 1, the proposed method cannot precisely locate the faulty switch, and it can only tell that the VD<sub>1</sub>/VD<sub>2</sub> leg is open circuited. In spite of this, the proposed method is still very applicable, because VD<sub>1</sub> and VD<sub>2</sub> have a much higher voltage and current rate comparing to VT<sub>x</sub>[24], VD<sub>1</sub>/VD<sub>2</sub> open-circuit faults happening in Phase 1 are almost impossible.

2) *Circuit Design*: By summarizing the above analysis, a fault diagnosis scheme is proposed and shown in Fig. 6. The operational amplifier circuit is designed to implement (9) and produce  $zcx(t)$ . The classic circuit composed of several Schmitt triggers is adopted by zero-crossing detection circuits ZCD1, ZCD2, and ZCD3 to produce zero-crossing pulse of  $zcx(t)$  defined in (11). The ZCS module is a simple zero-crossing

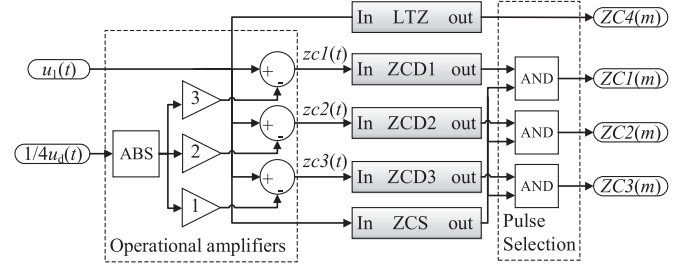


Fig. 6. Block diagram of fault diagnosis and location system.

detection circuit with an adjustable time delay function, it is designed to actualize (10). The LTZ module is a simple comparator circuit which compares  $u_1(t)$  with zero and generate pulse when  $u_1(t)$  is lower than zero.

### 3) Performance of the Proposed Method:

a) *Influence of noise*: The noise in the practical scenario is not negligible due to the strong electromagnetic interference introduced by electric machine and rectifier itself. Both input and output voltages are employed by the proposed method to obtain the fault feature. On the other hand, the positions of input and output voltages port of the rectifier are close to each other. If a parallel signal line is adopted in the practical application, the strength and the conduction path of the interference are similar for both input and output voltages. Interference will be neutralized in the difference of input and output, which will be weakened or even eliminated by the subtraction in the operational amplifier circuit. Moreover, by applying a proper threshold value of zero-crossing detection, the robustness of the proposed method to interference is ensured.

b) *Time delay*: The output current will drop slowly due to the inductive motor load after open-circuit faults happen. Consequently, the phase shift angle is adjusted by the control system and the variation of the phase shift angle is small. As a result,  $u_1(t)$  is barely affected by the control system for several working-cycles after faults happen. Moreover, the induced electromotive force caused by VD<sub>x</sub> open-circuit fault will stabilize in less than one working-cycle. Given all that, the several working-cycles after the occurrence of open-circuit fault and stabilization of the induced electromotive force can be regarded as a new steady state of the rectifier. All open-circuit faults can be detected within the working cycle when fault occurs, this is even before the faulty rectifier reaches its new steady state. Through the analysis above, the longest stabilizing time of  $u_1(t)$  arises when VD<sub>x</sub> open-circuit fault happens, faulty switches locating under that situation also can be done in less than one working cycle after the new steady state is reached.

## D. Fault Tolerance Control Strategy

1) *Operation Analysis of the Reconfigured Rectifier*: After open-circuit fault is located, it is possible to maintain the rectifier capacity by changing connection between transformer and

TABLE VI  
SWITCH POSITION OF THE FAULT TOLERANCE CONTROL STRATEGY

Faulty parts	K1	K2	K3	K4	K5
$VT_4/VT_3$	1	1	1	4	2
$VT_2/VT_1$	1	1	1	2	1
$VD_2/VD_1$	1	1	2	3	1
$VT_6/VT_5$	2	3	3	2	1
$VD_4/VD_3$	2	3	3	2	1

rectifier. The faulty rectifier is reconfigured by using remaining components. The proposed fault tolerance control strategy is present separately for each open-circuit fault. The rectifier can keep its full capacity without any adjustment when  $VT_2/VT_1$  open circuit.

a) *Under  $VT_4$  open-circuit fault conditions:* Adjust switch K5 to position 2 and K4 to position 4, winding  $a_1x_1$  is then connected to  $VD_1, VD_2, VT_1$ , and  $VT_2$ . The rectifier is turned into a two-stepped half-controlled bridge, and there is no need to adjust the original control signal. The output voltage can be regulated in full range, and only adjustment step-size in  $1/2u_d(t) \sim u_d(t)$  region is slightly increased. The reconfigured rectifier works just like the original one, operation principles are not discussed here.

b) *Under  $VD_2$  open-circuit fault conditions:* The rectifier is reconfigured by switching K3 in position 2 and K4 in position 3. Winding  $a_1x_1$  is connected to  $VT_1, VT_2, VT_3$ , and  $VT_4$ , meanwhile, by interchanging trigger pulse of  $VT_1$  and  $VT_2$ , the capacity of the rectifier remains intact.

c) *Under  $VT_6$  or  $VD_4$  open-circuit fault conditions:* When  $VT_6$  is an open circuit, K1, K2, K3, and K4 are switched to position 2, 3, 3, and 2, respectively. The reconfigured rectifier is now composited by winding  $a_1x_1, a_2x_2$ , and  $VD_1, VD_2, VT_1, VT_2, VT_3, VT_4$ .  $VD_3$  and  $VD_4$  freewheel the current.  $VD_4$  open-circuit fault conditions are similar, but  $VT_5$  and  $VT_6$  have to be fully triggered to freewheeling.

## 2) Completed Tolerance Control Strategy:

a) *State of switch sets:* Notice that, switches in the same leg are affected equally in each fault tolerance strategy. Take  $VT_3$  and  $VT_4$  as an example, when implementing the  $VT_4$  fault tolerance control strategy,  $VT_3$  is also excluded by the reconfigured rectifier. Therefore, under  $VT_3$  open-circuit fault conditions,  $VT_4$  fault-tolerance control strategy is equally applicable. Same inference can be applied to other switches. So, the completed fault-tolerance control strategy is shown in Table VI.

b) *Timing of the fault tolerance control strategy:* Because operations of five switch sets are involved in the reconfiguration process, the fault tolerance control strategy must be implemented after the current on all five switch sets are going down to zero to ensure operation synchronism, and to avoid unnecessary impulse voltage/current, so as to protect the remaining components of the system. After fault is located, the trigger signal is blocked by the controller, so the current will

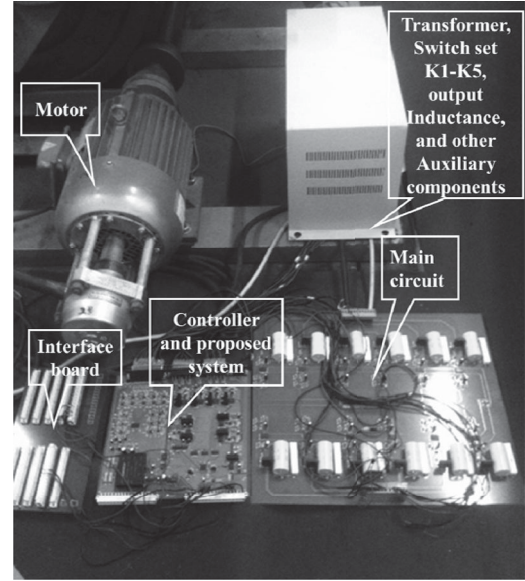


Fig. 7. Prototype of the experimental system.

TABLE VII  
KEY PARAMETERS OF THE PROTOTYPE

Components	Model	Components	Model
$VT_1$ - $VT_6$	BTA16-600B	$K1$ - $K5$	Composite by 9JQX-40F 2Z
$VD_1$ - $VD_4$	RHRP3060	Motor	Z2-42(340V/4kW)
11L/12L	0.028 H	Transformer	220V/190V X2, one of them have center tap
75R/76R	RxQ-100-750 $\Omega$ J		

take VDs as the freewheeling path, the secondary side of the traction transformer will not participate in current freewheeling, so all the five switch sets are ready for operation under zero-current condition. If one of  $VD_x$  is an open circuit, one of corresponding  $VT_x$  will not be able to cutoff. Take  $VD_2$  open circuit as an example,  $VT_4$  will endure continuous positive voltage during the faulty state, so  $VT_4$  cannot be cutoff no matter what the state of trigger signal is. Under this circumstance, the secondary side of the traction transformer is also not involved in current freewheeling, and the zero current condition for all five switch sets is ensured as well.

c) *Analysis of the electric stress:* it can be seen from the analysis above that, the largest voltage/current stress of switches is encountered under  $VD_4/3$  and  $VT_6/5$  open-circuit fault.  $VD_4$  is taken as an example to analyze the electric stress under the fault tolerance strategy. When the rectifier is under normal operation,  $1/4u_d(t)$  is switched by  $VT_{1(2)}$ , but after  $VD_4$  open-circuit fault tolerance strategy is implemented,  $1/2u_d(t)$  is switched by  $VT_{1(2)}$ . The situation on  $VT_{3(4)}$  is even worse, the voltage to be switched by  $VT_{3(4)}$  under normal operation is  $1/2u_d(t)$ , but  $u_d(t)$  is switched under the fault tolerance control strategy for  $VT_{3(4)}$ . Almost all electric stresses are doubled, and the highest is approximate 1400 V. Even though semiconductor devices in the original rectifier are rated as 2800 V minimal [24]. So, the proposed fault toler-

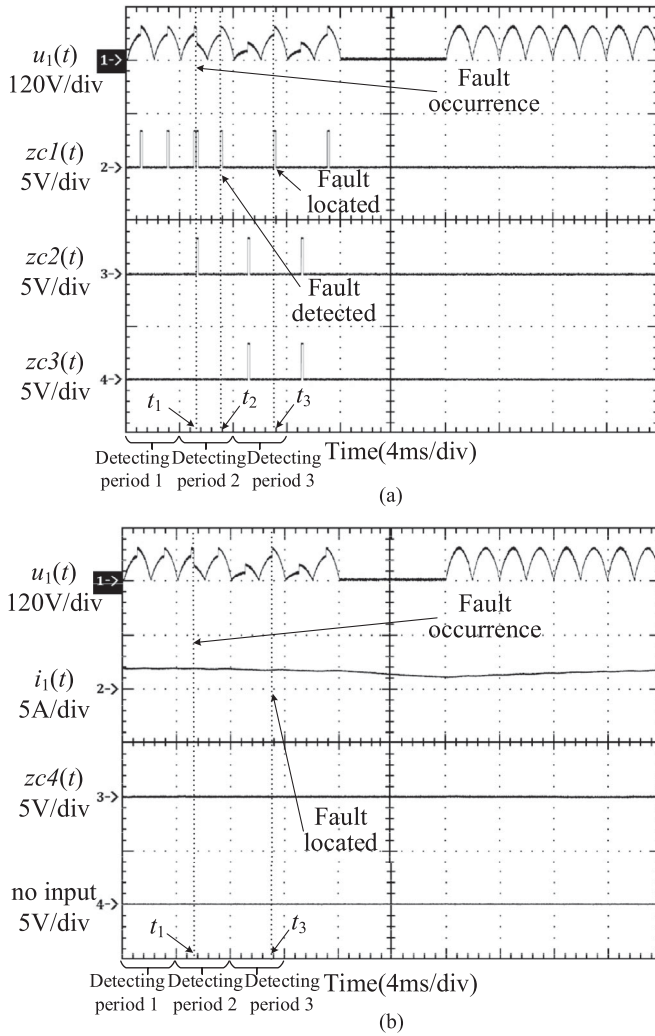


Fig. 8. Experimental result of  $VT_6$  fault in phase 3. (a)  $u_1(t)$ ,  $zc1(t)$ ,  $zc2(t)$ , and  $zc3(t)$  waveforms under  $VT_6$  fault. (b)  $u_1(t)$ ,  $i_1(t)$ , and  $zc4(t)$  waveforms under  $VT_6$  fault.

ance control strategy can achieve full output capacity without changing any original components.

#### IV. EXPERIMENT RESULT

To verify the proposed fault diagnosis method and the fault tolerance control strategy, a rectifier test bed with the same structure as the traction rectifier has been built, and ten relays have been added to the test bed to simulate open-circuit faults. Five switch sets have been added to reconfigure the faulty rectifier. The prototype is illustrated in Fig. 7. Key parameters of the test bed are shown in Table VII.

Experimental waveforms of  $VT_6$  open-circuit fault in phase 3 are shown in Fig. 8. Here, detecting period 1 to 3 are labeled for demonstration convenience.  $C(m)$  is [10001000] in detecting period 1.  $VT_6$  open circuit happens at  $t_1$  and causes  $u_1(t)$  to drop. Because the new steady state of the system is not reached,  $Z(m)$  is [21001000] and  $C(m)$  is [101001000] in detecting period 2, which is different from  $C(m)$  of the normal state, so

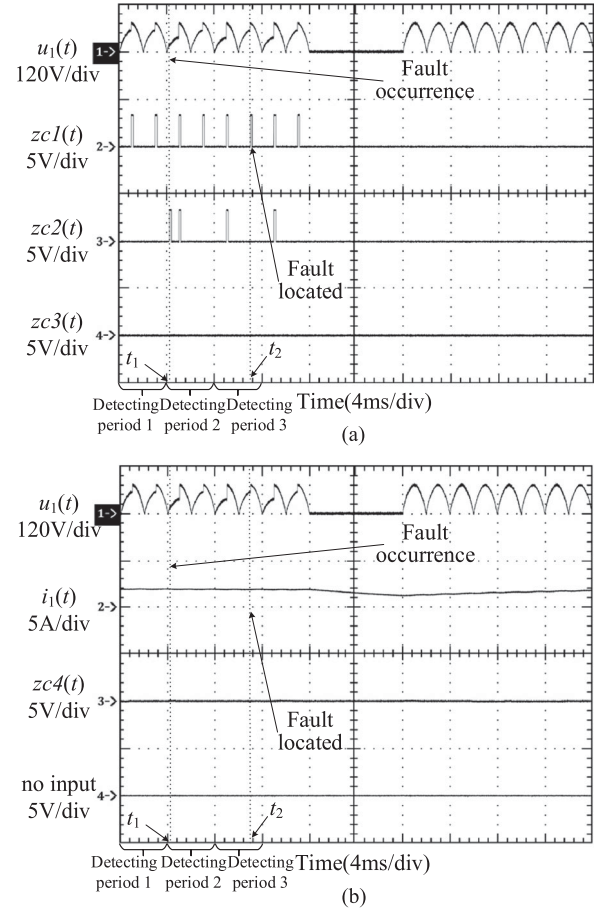


Fig. 9. Experimental result of  $VT_2$  fault in phase 3. (a)  $u_1(t)$ ,  $zc1(t)$ ,  $zc2(t)$ , and  $zc3(t)$  waveforms under  $VT_2$  fault. (b)  $u_1(t)$ ,  $i_1(t)$ , and  $zc4(t)$  waveforms under  $VT_2$  fault.

fault is detected at  $t_2$ .  $C(m)$  is [01101000] in detecting period 3, which indicates  $VT_6$  fault at  $t_3$ .

Waveforms of  $VT_2$  faults in phase 3 are shown in Fig. 9.  $Z(m)$  is [12001000] and  $C(m)$  is [100001000] in detecting period 2, which is different from  $C(m)$  of the normal state. After new steady state is reached in detecting period 3,  $C(m)$  equals to [11001000] and  $VT_2$  fault is located.

Waveforms of  $VD_3$  in phase 3 faults are shown in Fig. 10.  $VD_3$  open-circuit fault cuts off the current path, causing the induced electromotive force, which is generated by the inductive load. The induced voltage is large enough to make the synchronous transformer saturate at  $-600V$ . When the trigger pulse is blocked after fault detection, the load current has no path to go,  $VT_5$  cannot be cutoff immediately. The current passes through  $VD_1$ ,  $VD_2$ ,  $VD_4$ ,  $a_2x_2$ , and  $VT_5$ , and  $u_1(t) = 1/2u_d(t)$ .  $VT_5$  is cutoff until the current is reset at  $t_3$ , then K1–K5 can be switched at zero current condition, and the rectifier is rebooted, the load current starts to rise. The fault detection and locating process are similar to the two situations above.

Because the current continuously reduces in the process of diagnosis and fault tolerance control, the output current is lower than its set point. So after system is rebooted, the controller drives the rectifier working under full capacity to make the

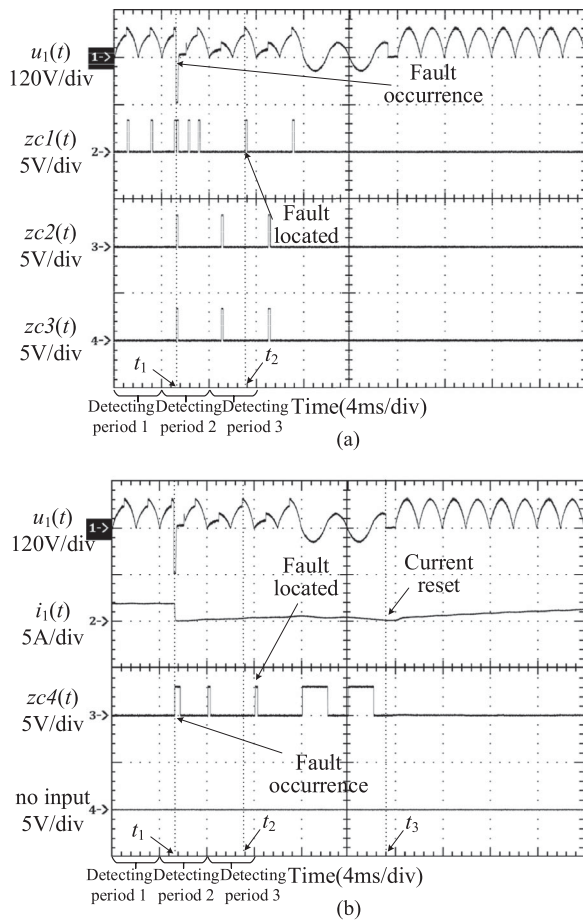


Fig. 10. Experimental result of  $VD_3$  fault in phase 3. (a)  $u_1(t)$ ,  $zc1(t)$ ,  $zc2(t)$ , and  $zc3(t)$  waveforms under  $VD_3$  fault. (b)  $u_1(t)$ ,  $i_1(t)$ , and  $zc4(t)$  waveforms under  $VD_3$  fault.

output current rise fast. Under this circumstance,  $C(m)$  is [00000000]. So, in practical diagnosis algorithm, the output voltage is combined with the vector  $C(m)$  as an auxiliary diagnostic signal. It also can be seen from waveforms that all open-circuit faults have been located in two working cycles, and the rectifier was rebooted after few working cycles when  $K1 \sim K5$  had been settled in suitable positions. During the reconfiguration period,  $K1 - K5$  do not have to switch under nonzero current condition.

## V. CONCLUSION

The new method can achieve diagnosis of any semiconductor device open-circuit fault in a short time period without either extra sensors or system structure changing. Moreover, the rectifier can maintain its full load capacity after being reconfigured according to the proposed fault tolerance control strategy. The validity and efficiency of the proposed fault diagnosis method and the fault tolerance control strategy are verified by experiment results. All the experimental results suggest that the new method is suitable for traction rectifier fault diagnosis and fault tolerance control. Due to the limitation of the experimental condition, the prototype has not been tested in the real traction

rectifier. The next step of this study is multiple semiconductor open-circuit fault diagnosis.

## REFERENCES

- [1] H. Chen and S. Lu, "Fault diagnosis digital method for power transistors in power converters of switched reluctance motors," *IEEE Trans. Ind. Electron.*, vol. 60, no. 2, pp. 749–764, Feb. 2013.
- [2] J. F. Marques, J. O. Estima, N. S. Gameiro, and A. J. Marques Cardoso, "A new diagnostic technique for real-time diagnosis of power converter faults in switched reluctance motor drives," *IEEE Trans. Ind. Appl.*, vol. 50, no. 3, pp. 1854–1860, May/Jun. 2014.
- [3] T. Kamel, Y. Biletskiy, and L. Chang, "Real-time diagnosis for open-circuited and unbalance faults in electronic converters connected to residential wind systems," *IEEE Trans. Ind. Electron.*, vol. 63, no. 3, pp. 1781–1792, Feb. 2016.
- [4] N. M. A. Freire, J. O. Estima, and A. J. M. Cardoso, "A voltage-based approach without extra hardware for open-circuit fault diagnosis in closed-loop PWM AC regenerative drives," *IEEE Trans. Ind. Appl.*, vol. 61, no. 9, pp. 4960–4971, Sep. 2014.
- [5] I. Jlassi, J. O. Estima, E. Khil, S. Khojjet, N. M. Bellaaj, and A. J. Marques Cardoso, "Multiple open-circuit faults diagnosis in back-to-back converters of PMSG drives for wind turbine systems," *IEEE Trans. Power Electron.*, vol. 30, no. 5, pp. 2689–2703, May 2015.
- [6] C. Brunson, L. Empringham, L. De Lillo, P. Wheeler, and J. Clare, "Open-circuit fault detection and diagnosis in matrix converters," *IEEE Trans. Power Electron.*, vol. 30, no. 5, pp. 2840–2848, May 2015.
- [7] W. Sleszynski, J. Nieznanski, and A. Cichowski, "Open-transistor fault diagnostics in voltage-source inverters by analyzing the load currents," *IEEE Trans. Ind. Electron.*, vol. 56, no. 11, pp. 4681–4688, Nov. 2009.
- [8] S.-M. Jung, J.-S. Park, H.-W. Kim, K.-Y. Cho, and M.-J. Youn, "An MRAS-based diagnosis of open-circuit fault in PWM voltage-source inverters for PM synchronous motor drive systems," *IEEE Trans. Power Electron.*, vol. 28, no. 5, pp. 2514–2526, May 2013.
- [9] U.-M. Choi, H.-G. Jeong, K.-B. Lee, and F. Blaabjerg, "Method for detecting an open-switch fault in a grid-connected NPC inverter system," *IEEE Trans. Power Electron.*, vol. 27, no. 6, pp. 2726–2740, Dec. 2011.
- [10] N. M. A. Freire, J. O. Estima, and A. J. M. Cardoso, "Open-circuit fault diagnosis in PMSG drives for wind turbine applications," *IEEE Trans. Ind. Electron.*, vol. 60, no. 9, pp. 3957–3968, Sep. 2013.
- [11] J. Baojun and A. Quntao, "A novel diagnostic technique for open-switch faults of inverters based on operating mode analysis," *Proc. CSEE*, vol. 32, no. 24, pp. 30–39, Aug. 2012 (in Chinese).
- [12] W. Qiang, W. Youren, Z. Zifu, and S. Zhe, "A diagnosis method for inverter open-switch faults of brushless DC motor driver systems," *Proc. CSEE*, vol. 33, no. 24, pp. 114–122, Aug. 2013 (in Chinese).
- [13] M. Trabelsi, M. Boussak, and M. Gossa, "PWM-Switching pattern-based diagnosis scheme for single and multiple open-switch damages in VSI-fed induction motor drives," *ISA Trans.*, vol. 51, pp. 333–344, 2012.
- [14] R. L. de Araujo Ribeiro, C. B. Jacobina, E. R. C. da Silva, and A. M. N. Lima, "Fault detection of open-switch damage in voltage-fed PWM motor drive systems," *IEEE Trans. Power Electron.*, vol. 18, no. 2, pp. 587–593, Mar. 2003.
- [15] X. Pei, S. Nie, and Y. Kang, "Switch short-circuit fault diagnosis and remedial strategy for full-bridge DC–DC converters," *IEEE Trans. Power Electron.*, vol. 30, no. 2, pp. 996–1004, Feb. 2015.
- [16] M. Shahbazi, E. Jamshidpour, P. Poure, S. Saadate, and M. R. Zolghadri, "Open-and short-circuit switch fault diagnosis for nonisolated DC–DC converters using field programmable gate array," *IEEE Trans. Ind. Electron.*, vol. 60, no. 9, pp. 4136–4147, Sep. 2013.
- [17] M. Rigamonti, P. Baraldi, E. Zio, D. Astigarraga, and A. Galarza, "Particle filter-based prognostics for an electrolytic capacitor working in variable operating conditions," *IEEE Trans. Power Electron.*, vol. 31, no. 2, pp. 1567–1576, Feb. 2016.
- [18] A. B. Youssef, S. K. El Khil, and I. Slama-Belkhdja, "State observer-based sensor fault detection and isolation, and fault tolerant control of a single-phase PWM rectifier for electric railway traction," *IEEE Trans. Power Electron.*, vol. 28, no. 12, pp. 5842–5854, Dec. 2013.
- [19] A. E. Ginart, D.W. Brown, P. W. Kalgren, and M. J. Roemer, "Online ringing characterization as a diagnostic technique for IGBTs in power drives," *IEEE Trans. Instrum. Meas.*, vol. 58, no. 7, pp. 2290–2299, Feb. 2009.

- [20] B. Ji, V. Pickert, W. Cao, and B. Zahawi, "In situ diagnostics and prognostics of wire bonding faults in IGBT modules for electric vehicle drives," *IEEE Trans. Power Electron.*, vol. 28, no. 12, pp. 5568–5577, Mar. 2013.
- [21] Y. Song and B. Wang, "Survey on reliability of power electronic systems," *IEEE Trans. Power Electron.*, vol. 28, no. 1, pp. 591–604, Apr. 2012.
- [22] R. L. de Araujo Ribeiro, C. B. Jacobina, E. R. C. da Silva, and A. M. N. Lima, "Fault-tolerant voltage-fed PWM inverter AC motor drive systems," *IEEE Trans. Ind. Electron.*, vol. 51, no. 2, pp. 439–446, Apr. 2004.
- [23] W. Dong, X. Bai, N. Zhu, Z. Zhou, H. Li, and W. Li, "Research on fault diagnosis and fault tolerant control of active power filters," *Proc. CSEE*, vol. 33, no. 18, pp. 65–74, Jun 2013 (in Chinese).
- [24] Y. Zhang, Y. Liu, and L. Zhu, *SS4 Locomotives*, 1st ed. Chin. Railway Press, Beijing, China, 1998, pp. 210–230.



**Cheng Shu** was born in Changsha, China, in 1981. He received the B.E. degree in automation from the East China University of Science and Technology, Shanghai, China, in 2003, and the M.S. and Ph.D. degrees in electrical engineering from Central South University, Changsha, China, in 2006 and 2011, respectively.

Since 2007, he has been a Permanent Researcher with the Institute of Rail Transport and Electric Traction Technology, and is currently a Lecturer at the School of Traffic and Transportation Engineering, Central South University. His main research areas include fault diagnosis and fault tolerant control of electrical drivers and electric traction control technology.



**Li Wei** was born in Xingning, China, in 1969. He received the B.E. degree in automation from the South China University of Technology, Guangzhou, China, in 1992, and the Ph.D. degree in traffic and transportation engineering from Central South University, Changsha, China, in 2012.

Since 1992, he has been an employee with CSR Zhuzhou Institute Co., Ltd., Zhuzhou, China, and is currently a Professor at the School of Traffic and Transportation Engineering, Central South University. His main research area is the network control

system.



**Ding Rong-Jun** was born in Yixing, China, in 1961. He received the B.E. degree in electric locomotives from Southwest Jiaotong University, Leshan, China, in 1984, and the M.S. and Ph.D. degrees in control engineering from Central South University, Changsha, China, in 1998 and 2008, respectively.

Since 1984, he has been an employee with CSR Zhuzhou Institute Co., Ltd., Zhuzhou, China, and is currently an Academician at the Chinese Academy of Engineering, Beijing, China. His main research areas include ac drive and network control system.



**Chen Te-Fang** was born in Lianyuan, China, in 1957. He received the B.E. degree in automation from the Dalian University of Technology, Dalian, China, in 1981, and the M.S. and Ph.D. degrees in electrical engineering from Central South University, Changsha, China, in 1991 and 2005, respectively.

Since 1982, he has been a permanent Researcher with the Institute of Rail Transport and Electric Traction Technology, and currently a Professor at the School of Traffic and Transportation Engineering, Central South University. His main research areas include fault diagnosis and fault tolerant control of electrical drivers and electric traction control technology.